Imperial College London

Imperial College London

TWO STAGE SOLID FUEL SUPERSONIC ROCKET

DESIGN REVIEW

Authors:
Cameron Morrison, Patryk Kulik, Nikhil Dawda, Edward Brown, Jonas Sinjan,
Joshua Rodgers, Gregorius Campman, Thiago Pinto, Orkid Ramekaj

This project is presented by the High Powered Rocketry group of the Imperial College Space Society

Abstract

This report details the design methodology, and manufacturing methods of a two stage rocket. The rocket entails various altimeters to determine whether the goal of the project is met: to break the sound barrier. The rocket is largely made up of composite materials in an aim to increase the thrust to weight ratio whilst maintaining structural integrity at high aerodynamic loads. The rocket will be powered by two solid fuel motors, I-class, and J-class.

Contents

Nomenclature

Roman Symbols

C_D	drag coefficient	–
M	mach number	–
R	radius of the nose cone as a function of x	m
x	distance for nose cone profile geometry	m

1 Introduction

1.1 Who are we?

The team is made up of first, second, and third year students from The Aeronautical engineering department, and the Physics department at Imperial College London. The project is housed within the Imperial College Space Society: High Powered Rocketry has always existed as the only space related student project at Imperial to have launched a rocket. As such it is the only project that allows students to apply knowledge of supersonic flows, and manufacturing methods. Thus the goal of this project is the most ambitious the society has had, to create a successful supersonic rocket, and recover it. The foundations of the project date back to 2018, where various components were designed, leading us to where we are now, in our final manufacturing push, and searching for a launch site.

1.2 What are we making?

The rocket is made up of two stages, in an effort to optimise the flight path, and utilise the engines available. The first stage will bring the rocket to Mach XXXX, before super-critical flow affects the aerodynamics of the rocket. At this point the second, much more powerful motor, will blast the rocket through the sound barrier, to a satisfying crack, and approach a final velocity of (430m/s) approximately Mach 1.3 at an altitude of 13,000 ft. This report aims to detail the design processes, and the manufacturing methods used throughout this project.

2 Body Tube

2.1 Body Tube Design

The rocket tubing for the entire rocket was kept at a constant diameter to relieve the need for a cowling at the staging joint, thus the rocket has a constant diameter from the edge of the nose cone to the motor nozzle. This enabled the re-use of designed components, such as the fin mount, which is similar for both stages.

2.2 Body Tube Material

The material used for this component is pre-manufactured carbon fibre tubing, with a fine weave. Pre-manufactured tubes were used to ensure the surface finish was up to standard, as the manufacture of our own carbon fibre components may lead to uncertainties in the structural properties. Further to this, any small disturbances in the surface would result in Mach waves, and plausibly some Oblique shock waves, which would massively increase the drag acting on the rocket and could lead to instabilities.

2.3 Structural Integrity Testing of the Tube

To test the structural integrity of the rocket, the load results (from the simulations detailed later) were utilised on a Finite Element Analysis model. This entailed loading a carbon fibre tube with 25g's, approximately $250Kg/m^2$. This force is huge, so the test was run, using a fully constrained base of the tube and the force applied to the upper surface, and showed a 3mm deflection. This was deemed

suitable for the current centring ring design. The stress within the tubing is well below the critical value, and as such this material is ideal for the body tube. The test was completed using a multi-pass adaptive method with automatic mesh generation, using *Creo Simulate*.

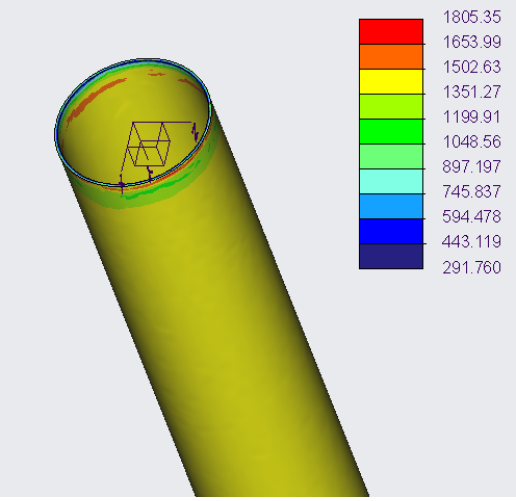

Figure 1: Stress (MPa) experienced at the top of the tube under maximum forces.

2.4 Attachment of Tubing to Fin Mount

DISCUSS GLUEING THE MOUNT TO THE TUBE - TALK ABOUT THE SMART DUDE AND WHAT HE SAID

3 Staging System

The approach taken for designing the staging system, as one of the critical parts of the rocket required for success, was that of simplicity and predictability. The approach chosen was to use an overlapping tube approach as this is well documented, and has a history of success with other multi-stage model rocket projects.

3.1 Staging Design

The simple principle behind the staging system is essentially that the two stages overlap and ignition of the upper stage motor, through it's exhaust pushing the bottom stage within the confined space, pushes the two stages apart. To prevent incineration of the lower stage's parachute during this separation, excess wadding is used.

3.2 Staging Manufacture

To achieve the overlap between the stages we plan to 3D print an interstage component in a carbon fibre reinforced Onyx polymer. This component is essentially a hollow tube that is secured to the inside wall of the bottom stage body tube via a strong adhesive which the upper stage body tube can slide over, with the upper stage rocket motor in the centre. The fit required for this tube with the

upper stage is a reasonably loose friction fit, this is to ensure that the rocket remains sufficiently rigid when the stages are together to mitigate excitement of any dynamic modes whilst also providing a loose enough fit for the force from the upper stage motor to be sufficient to push apart the stages. Whilst not required, to further ensure that staging occurs seamlessly the inner and outer faces of the interstage component will be covered in non-flammable lubricant before flight to minimise the sliding friction that staging requires overcoming.

3.3 Structural Considerationsof Staging

To help achieve rigidity of the vehicle pre-separation and to ensure that the staging motion occurs in a linear fashion, so as to keep the vehicle on course, the overlap between the stages needs to be of sufficient length. For our vehicle we have opted to make the interstage component 20cm long. This consists of 10cm overlapped within the inside of the lower stage body tube, rigidly attached via a strong adhesive, and 10cm overlapped within the upper stage body tube. To achieve this a slight compromise had to be made to the geometry of the interstage component to prevent interference with the lowest upper stage engine centring ring. This compromise is that halfway into the overlap with the upper stage, the interstage component ceases to be a hollow tube and instead has cut-outs for the modified centring ring to fit through. Figure 2 shows the designed interstage component.

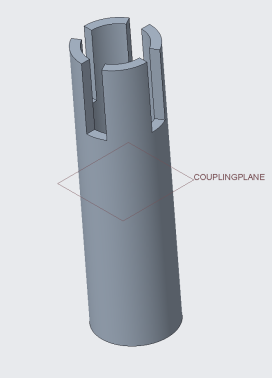

Figure 2: A CAD render of the interstage component. The plane visible in the render indicates the plane where the two outer body tubes will meet

Whilst the interstage component will be made of a strong fibre reinforced polymer, it will not be carrying the bulk of the longitudinal force from the lower stage motor through the rocket to the upper stage as this is the job of the body tubes. To ensure that this is the case, care will be taken during manufacturing to ensure that the upper faces of the interstage component are not in contact with any of the upper stage's centring rings.

3.4 Safety Mechanism

The team is aware that the staging presents the most dangerous stage of the flight regime, and as such there is a built in safety mechanism to ensure that in the event of a decoupling failure, the rocket can still be safely recovered. In the event that the two rocket halves fail to separate, the interstage and outer body tubes will have two small holes drilled on opposite sides to ensure that exhaust gases are

able to ultimately escape from within. If the upper stage motor fails to ignite then the upper stage will either safely remain connected with the lower stage, or more likely will naturally separate allowing for each stage to be recovered by parachute and re-flown to attempt another launch.

4 Fin Design

4.1 First Stage Fin

4.1.1 Fin Geometry

The set of three fins attached to the bottom stage of the rocket are optimised for flight during the initial subsonic regime. They are mounted to the body of the rocket in a radially symmetric orientation (three fins equally spaced). A "clipped delta" geometry was chosen over a more aerodynamically efficient elliptical design due to the former being significantly easier to manufacture, whilst maintaining the aerodynamic stability required to bring the rocket to the point of first stage decoupling. Based on historical data and common practice within amateur rocketry, the tip chord length (114mm) was set to be half that of the root chord length (57mm) so as to guarantee a balance of structural integrity and aerodynamics. The fin aspect ratio was optimised by considering such factors. Through iteration, the optimal aspect ratio value was found to be just over one. Therefore, to ensure this condition, the fin semi-span was designed to be equal to the root chord length.

4.1.2 Fin Manufacture

As will be described in the second stage fin manufacture, this component is made of lasercut Aluminium.

4.1.3 Fin Mount Design

The fin mount effectively sandwiches the aluminium fins on each side for XXmm, which was shown to withstand the bending moments acting at the root at any given reasonable flight path. Three M3 bolts pass through the aluminium fin, fixing it inside the mount.

4.1.4 Fin Mount Manufacture

This mount was manufactured through additive manufacture. The resulting mount is made up of a a carbon fibre reinforcement, with closed loops in the axial direction. Twisting of the fins results in an axial stress, thus the reinforcement in this direction ensures the mount maintains structural integrity. The matrix surround the reinforcement is Onyx, which contains additional small portions of carbon fibre randomly distributed to improve the isotropic properties of the mount.

4.2 Second Stage Fin

To stabilise the supersonic stage, fins were optimised for the transonic-supersonic regime, mounted to the base of the second stage.

4.2.1 Fin Geometry

The fins represent a smooth ogive-delta shape. This shape is optimal for low supersonic and transonic speeds. The sweep delays shock wave formation as the relative angle of the flow is reduced, thus reducing the effective Mach number the fin experiences.

$$M_{\text{effective}} = M_{\text{cruise}} \sin\theta \tag{1}$$

The increase in sweep angle at the root of the fin provides two benefits, firstly it has the structural benefit of a greater length clamped into the fin mount. Additionally this angle allows the root to stall before the tip, increasing the stability of the rocket.

The area of the fin was determined through the use of open rocket (stability consideration is discussed in a subsequent section), where a model of the rocket was built up, and the static margin was determined for a given fin area. This area was used to scale the equation of the curve, shown in equation XX. this curve was shown to closely follow the ogive-delta shape. The use of this equation allowed for calculations relating to area, stability, and forces to be more easily calculated with analytical integration, rather than numerical methods.

4.2.2 Second Stage Fin manufacture

The manufacture of the fins was outsourced to Essex Lasers Ltd. as the facilities available to use did not allow a variable swept fin geometry. Thus the fin was laser cut allowing a precise and sharp edge. The fins were made of aluminium of 1mm thickness. (discuss temp!!!!!). The Aluminium is capable of withstanding shock formation and the aero-thermal heating.

$$y = \frac{e^x}{1 + e^x} \tag{2}$$

4.2.3 Fin Mount Design

The design of the second stage fin mount follows the exact same design principles of the first stage fin mount. This is a benefit drawn from the standardised diameter along the length of the two stages.

5 Centring Rings

This is the component used to centre the engines within their respective stages for correct alignment of the thrust.

5.1 Centring Rings Design

Multiple centring rings were be placed along the engine, at locations given in tables 2 and 3. The dimensions of the rings are given in table 1.

Dimension	length / cm
Outer diameter	5.5
Inner diameter	4.2
Thickness	0.9

Table 1: Centring Ring Dimensions

Location	distance / cm
1	0
2	10
3	20
4	36

Table 2: Centring ring locations for the first stage, with reference to the bottom of the tube and bottom of centring ring

Location	distance / cm
1	3
2	10
3	20
4	30
5	35

Table 3: Centring ring locations for the second stage, with reference to the bottom of the tube and bottom of centring ring

5.2 Centring Rings Manufacture

This was done on site, using the Imperial College Hack Space facilities. The rings were laser cut from 3mm plywood boards, to form layers which were sandwiched together using a PVA based adhesive. These manufactured centring rings were then bonded to the inner tube using an epoxy resin.

6 Nose Cone

After extensive research of possible nose cone geometries, as well as looking into the viability of computationally determining the optimal nose profile, the aerodynamics team have determined that use of a pre-optimised profile would be the best way forward in terms of time and final effectiveness.

6.1 Nose Cone Geometry

To determine the best geometry, a Honors Thesis from University of Alabama[1] was used, which allowed for a comprehensive comparison of different nose geometries in the Mach 0.3 - Mach 1.7 regime (which strongly overlaps with a our predicted velocity range). In the end, the Von Kármán Haack series was determined to give the best result in terms of minimising total drag experienced during flight. This nose cone is defined using Eqs. (3) and (4), which have been derived using linearised flow theory with the explicit objective of minimising drag.

$$\theta(x) = \arccos(1 - \tfrac{2x}{L}) \tag{3}$$

$$R(x) = \tfrac{R_{\text{base}}}{\sqrt{\pi}} \sqrt{\theta(x) - \tfrac{\sin 2\theta(x)}{2}} \tag{4}$$

To provide a visual output of the above equations, the nose cone has been initially plotted in python (see Fig. 3a), as well as modelled in PTC Creo and 3D printed to test the design feasibility - see Fig. 3b.

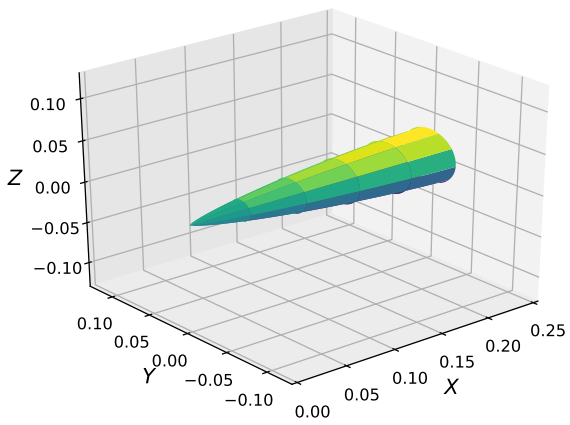

(a) Three-dimensional Python model of Von Kármán nose cone used for the rocket

(b) 3D print of the nose cone in 1:3 scale

Figure 3: Nose cone design

6.2 Nose Cone Manufacture

The Nose cone materials largely revolved around the aero-thermal heating effects, and the radio transparency. The control electronics are designed to sit within the nose cone, in an effort to optimise the volume of the rocket.

7 Propulsion

The rocket will be powered by two solid fuel motors. The motors for the upper (second) stage, and the lower (first) stage are J-class and I-class respectively. The motor parameters are detaile din the table below.

8 Drag Estimation

Given that the rocket will operate in sonic, transonic and supersonic regime, we expect wave drag to give a relatively large contribution to the total drag force of the rocket. Because of the difficulty in theoretical modelling of wave drag, as well as lack of simple models applicable for our implementation, it was initially decided by the aerodynamics team to attempt solving this problem using computational implementation Euler equations and numerical methods. However, after consulting many lecturers from the Imperial Aeronautics Department the team has shifted their focus towards computational implementation of experimentally established equations. To achieve this, a Ballistic Research Laboratories report[2] was used in combination with Kopal tables for Supersonic Flow Around Yawing Cones[3]. The exact method of implementation is presented in Section A in the form of Python code

Motor Parameters	Upper Stage:	Lower Stage:
Motor:	J357	I540WT
Make	Cesaroni	Cesaroni
Specific Impulse (Ns)	657	635
Average Thrust (N)	373	548
Max Thrust (N)	514	626
Burn Time (s)	1.76	1.16
Launch Mass (g)	601	598
Empty Mass (g)	264	269
Motor Diameter (cm)	3.8	3.8
Motor Length (cm)	36.7	36.7

Table 4: Rocket and Motor Parameters

and the final predicted drag coefficient value at the most critical point (Mach 1.2 and height of 2,100 m) was obtained as approximately 1.36. Given will likely form the upper-bound of the drag coefficient during flight, to ensure that supersonic flow is reached, for the required thrust calculation it was assumed that $C_D = 1.36$ throughout the entire flight.

9 Conceptualisation of Telemetry and Stage Separation Systems

The combination of both on-board telemetry, as well as stage separation will be implemented through two modules. One inside the nosecone (NAM - Nosecone Avionics Module), and another placed at the top of the first stage (SAM - Secondary Avionics Module).

NAM will be responsible for; a) Ensuring telemetry logs of the supersonic stage, in terms of acceleration, orientation, as well as GPS co-ordinates. b) Release of the main second stage descent parachute using a barometric altimeter. c) Broadcasting location of the second stage as it descends and lands.

SAM will be responsible for; a) Ensuring telemetry logs of the subsonic stage, in terms of acceleration, orientation, as well as GPS co-ordinates. b) Release of the main first stage descent parachute using a barometric altimeter. c) Broadcasting location of the first stage as it descends and lands. d) Precise timing of the supersonic stage separation using a precision timing module.

All these functions and sensors will be tested in some capacity before launch, hopefully inspiring confidence that they will work correctly during flight. However it will be especially difficult to test stage separation in the trans-sonic regime - although this can easily be tested from an electronics standpoint. We will also verify to the best of our ability, that the sensors operating limits are within our mission parameters.

It is our intention to use multiple levels of redundancy in certain elements of the avionics, for instance multiples SD card readers to measure data, perhaps dual/triple barometric altimeters and gyroscopes as well as multiple wires to enable ignition of the supersonic stage motor.

Both modules will be housed in lightweight carbon reinforced resin frames that minimise launch mass and provide more resilience upon landing than an acrylic/fibreglass frame would. SAM will be wrapped in a large amount of fire retardant material, and will be daisy-chained between the first stage and parachute. NAM will have equal pressure to the environment via ventilation holes drilled in the bottom of the nosecone cap. The nosecone will be linked to the second stage, with the parachute latching in-between the two.

For broadcasting location, we are still researching the viability of certain options based on cost, legal spectrum usage requirements and range. Currently it seems like viable options would be to broadcast location using a low power antenna, or utilise a low power GSM antenna depending on the mobile phone coverage at the launch site. Lastly, if it proves unfeasible, we could empirically estimate where both stages would land and search for them by sight. This is a last resort.

Powering both modules is likely to be via a small USB rechargeable battery pack.

10 Rocketry Simulations and Stability

To ensure the rocket safely completes the designed mission profile, various peices of software in conjunction with tailored codes were used.

10.1 Stability Margin

According to rocketry literature, historical data, and the advise from other rocketry enthusiasts; it was suggested that the stability margin of the rocket for supersonic rockets be placed between 1.7 and 2.0. As this is the case and taking into account the supersonic fin design, a stability margin of 1.8 was chosen. This will allow for the rocket to hold directional stability but not remain weather cocked at high speeds. This should help maintain the rockets initial vertical direction. The value is a play off between manoeuvrability and stability.

To ensure there is a not a huge jump in stability, the top and bottom stage stability margin was made similar. This would hopefully provide a smoother transition at separation.

10.2 *Rocksim* Simulations

The table below, holds the centre of gravity (COG) and centre of pressure (CP) positions for launch and after staging, along with its associated stability margin. The COG and CP values were measured in relation to the front most part of the nosecone. *Rocksim* was used to obtain these parameters.

	COG (cm)	CP (cm)	Stability margin
Launch	106	117	1.81
After Staging	70.4	80.8	1.81

Table 5: Stability parameters during Launch and staging.

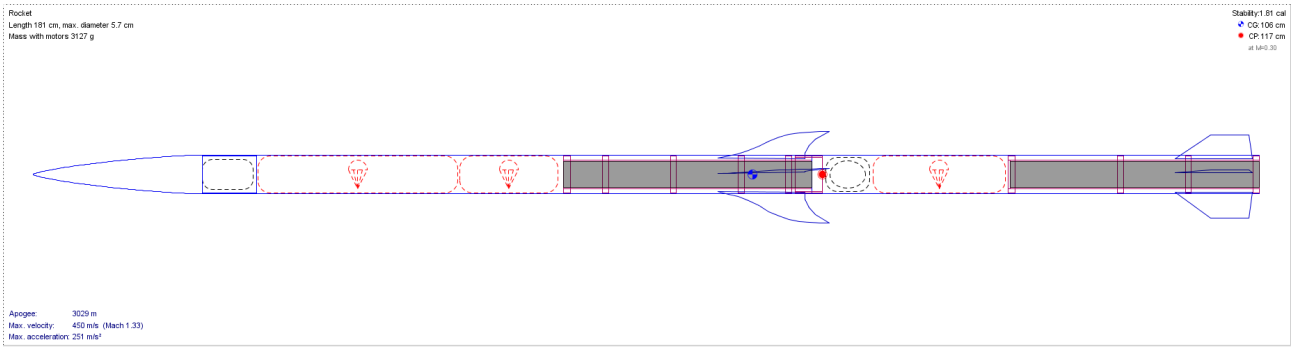

Figure 4: The Rocksim model of our CP (red) and COG (blue) positions on the rocket in it's launch configurations

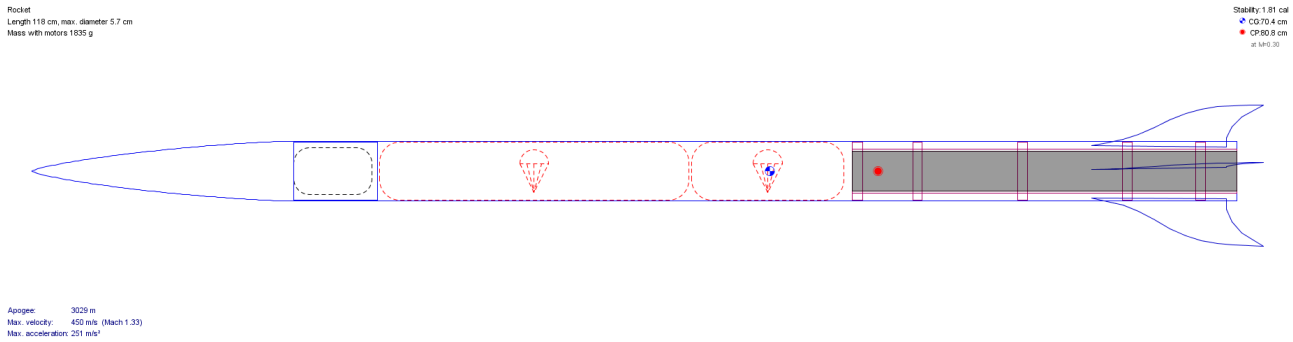

Figure 5: The COG and CP configuration for the upper stage rocket directly after staging

A visual representation of this data is shown in figure 2 and figure 3
With the stability of the rocket designed, we can focus more on the predicted rocket data and flight trajectories. With the following rocket parameters and motor configurations in Table 5; the predicted first stage flight data can be accurately given by *Rocksim*. This is because we are still within and below the speed regime of Mach 0.3; the point at which *Rocksim* can use in-compressible flow assumptions in its calculations.

Global Rocket Parameters	
Total Length (cm)	181
Max Body Diameter (cm)	5.7
Mass: with Motors (kg)	3.13

Local Rocket Parameters	Upper Stage:	Lower Stage:
Total Length (cm)	118	63
Max Body Diameter (cm)	5.7	5.7
Mass: with Motors (kg)	1.835	1.292
Mass: After Burnout (kg)	1.498	0.963

Above Mach 0.3, the assumption that flow is incompressible does not hold (Density change reaches approximately 5%). With increasing speed (and hence Mach number), and expecially as the rocket moves into the transonic regime, compressibility effects must to be taken into account and thus the drag coefficient contribution due to wave drag is calculated. The Rocksim image below shows the estimated velocity, displacement and acceleration profiles of both stages up to M=0.3, where

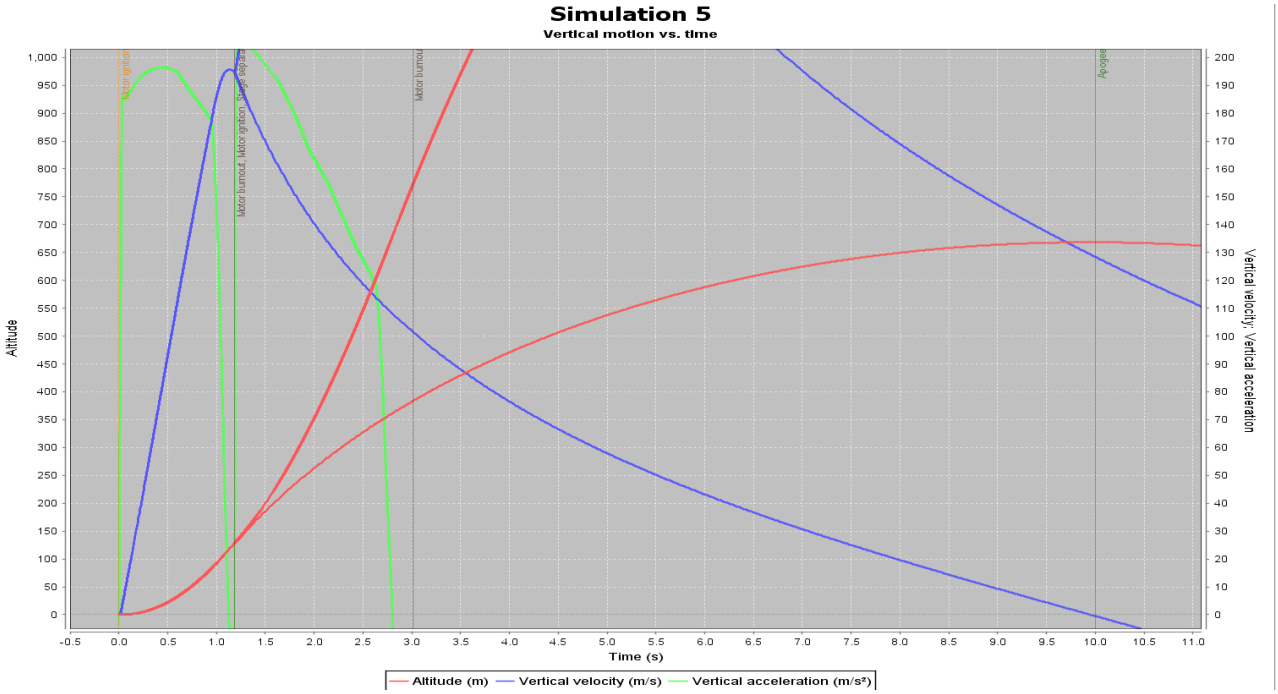

Figure 6: The Rocksim model trajectory profiles in assumed in-compressible flow

As we can see from the graph; staging has been aligned to coincide with the velocity beak of the entire rocket. The implications are that we will minimise the loss of velocity imparted onto the upper stage after separation and therefore, we improve the chance of breaking the sound barrier. Another profound implication is that the staging ignition system will have to fire approximately 0.1 to 0.15 seconds before this point; to ensure the second stage motor becomes thrust producing at the time we hit the velocity peak. This control sequence is integrated within our electronics system.

10.3 Aero-Thermal Heating

During flight we would expect that the hottest part of the rocket body, as a result of compressibility effects, would be at the tip of the nosecone. By taking the wall deflection angle of our nosecone to be δ_{wall} =6.50° we can calculate what the estimated maximum temperature our rocket will encounter at a proposed altitude of 1200m. This is where we expect to hit the maximum velocity. Using oblique shock relations and shock tables, we can see that there is a transition between Mach 1 to Mach 1.24 from a bow shock to an attached oblique shock. Using this information we can estimate the max temperature to be around 380 K. This information was useful in material selection for the nose cone. The nose cone must have a glass transition temperature greater than this.

11 Trajectory Simulation

A small python script was written to give an estimation of the ΔV, apogee height, and coast time. Since the set of differential equations that govern this system have a dynamic mass, the equations cannot be solved for analytically. An estimation for the average mass during each stage was made by taking half the propellant mass that was ignited during thrust[4].

	Estimation (2dp)
Coast Time	19.25s
$\Delta V_{\text{first stage}}$	97.06ms^{-1}
ΔV_{max}	672.53ms^{-1}
Apogee Height	3965.86m

Table 6: Estimations of Trajectory Properties

The $\Delta V_{firststage}$ estimation seemed reasonable however the ΔV_{max} appeared to be rather large. Upon comparison to RockSim , it output a value of roughly $430ms^{-1}$, which appeared to be more appropriate. The final apogee height of roughly $4000m$ agreed with RockSim. The delay on the second stage motor was $17s$, which agrees with this estimation for the coast time of $19.25s$. Since this is a large rocket, relative to model rockets, and the mass changes considerably during flight, an attempt to solve the differential equations numerically will be made to estimate more accurate numbers for the trajectory.

12 Project Roles

Project Manager - Cameron Morrison
Head of Engineeing - Nikhil Dawda
Aerodynamicist - Patryk Kulik
Internal Structures - Gregorius Campman
Head of Control Systems - Joshua Rodgers
Staging Mechanism - Edward Brown
Flight Physics - Jonas Sinjan
First stage fins - Thiago Pinto
Head of Manufacturing - Orkid Ramekaj

References

[1] Chad O'Brien. *An Investigation of Drag on the Haack Series Nose Cones through Subsonic and Supersonic Mach Regimes*. PhD thesis, The University of Alabama in Huntsville, 2014.

[2] H. P. Hitchcock. On Estimating the Drag Coefficient of Missiles. Technical report, Ballistic Research Laboratories, 1966.

[3] Zdenek Kopal. Tables of Supersonic Flow Around Yawing Cones. Technical report, Massachusetts Institute of Technology, 1947.

[4] Randy Culp, August 2008. URL: `http://www.rocketmime.com/rockets/multistg.html`.

Appendix A Python script used for drag coefficient estimation

```python
import numpy as np
import matplotlib.pyplot as plt
from scipy.integrate import simps
from scipy.interpolate import interp1d


def Parameters(atm_height, R):
    T_0 = 288.15
    g_0 = 9.81
    P_0 = 101325
    rho_0 = 1.225
    T1 = 216.65
    if atm_height <= 11000:
        T = T_0 - 0.0065*atm_height
        P = P_0 * (1 - (0.0065 * atm_height) / T_0) ** (g_0/(0.0065*R))
        rho = (rho_0 *P*T_0) / (P_0 * T)
    elif atm_height > 11000 and atm_height <= 20000:
        T = T_0 - 0.0065*11000
        P1 = P_0 * (1 - (0.0065 * 11000) / T_0) ** (g_0/(0.0065*R))
        P = P1 * np.exp(- (g_0 * (atm_height - 11000)) / (R * T1))
        rho = (rho_0 * P * T_0) / (P_0 * T)
    # else:
    #     T = T_0 - 0.0065*11000 + 0.001*(atm_height-20000)

    return (T, P, rho)



# Definitions
M = 1.2
atm_height = 2100
R = 287 # air constant
T, P, rho = Parameters(atm_height, R)
d_b = 0.057  # diameter of base in meters
gamma = 1.4
d = 0.057  # caliber of the missile
h = 0.25  # height of the nose
flow = 'laminar' #check with cd vs re of rocket
mu = 1.716 * (10**(-5)) * ((T/273.15)**1.5) * (273.15 + 110.4)/(T + 110.4) #
 ↪  sutherland's law for viscosity
```

```
a = (gamma * R * T)**0.5
U = M * a # velocity
height_rocket = 1.54
Re = (rho * U * height_rocket) / mu # Reynolds number
S_wet = (np.pi * d) * height_rocket


############################################################
# Nose drag coefficient:

# Semi-apex angle of inscribed cone
theta_s = np.rad2deg(np.arctan(d / (2 * h)))

# Radial velocity
u_s = 0.425

head_correction = 0  # ?

K_DC = 0.0888

############################################################
# Base drag coefficient:

# Pressure ratio = Pressure at base / Atmospheric Pressure
Pressure_ratio = 1 - 0.3086 * M + 0.1085 + 0.02411 * M ** 2

# A_b is equal to the base area
A_b = (np.pi / 4) * d_b ** 2

K_DB = (1 - Pressure_ratio) * A_b / (gamma * d * M ** 2)

############################################################
# Wave drag on fins coefficient:

t = np.arange(-6, 6.001, 0.001)
span = 5*(np.exp(0.5*t))/(1+np.exp(0.5*t))
span_distr = interp1d(t, span, kind = 3)

linear_span = np.arange(span_distr(-6), span_distr(6), 0.001)
chord = 2 * np.log(linear_span/(5 - linear_span))
chord_distr = interp1d(linear_span, chord, kind = 3)

```

```
82
83  # span of fins
84  s = span_distr(6) - span_distr(-6)
85
86  # mean aerodynamic chord of fins
87  fin_area = simps(span, t) * (0.0001)
88  c = (2 / fin_area) * simps(chord**2, linear_span)
89
90  # Aspect ratio of fins
91  AR = 0.25 * ((s**2) / fin_area)
92
93  # Wedge angle of fins
94  beta = 0.5586
95
96  # Seep back angle of fins
97  # sweep =
98
99  # B parameter
100 B = (M**2 - 1)**0.5
101
102 C_DW = ((beta**2) / B) * (1 - 1/(AR*B))
103
104 K_DW = C_DW * (fin_area/(d**2)) #check S here
105
106
107 ###############################################################
108 # Friction drag coefficient:
109
110 # apparently it should be calculated for both flow regimes and average taken
111 # also the main body should be done separately from the fins
112
113 lam = (((gamma - 1) * 0.5 * M**2) / (1 + (gamma - 1) * 0.5 * M**2))**0.5
114 if flow == 'turbulent':
115     temp = 1
116     C_f = 0
117     while abs(temp) > 10**(-3):
118         C_f += 0.00001
119         temp = np.log10(Re) - (0.242 * (C_f**(-0.5)) * ((1 - lam**2)**(0.5)) *
          ↪  (lam**(-1)) * (np.arcsin(lam)**(-1)) - np.log10(C_f) - 1.26 * np.log10(1
          ↪  - lam**2))
120 else:
121     C_f = 1.328 * Re**(-0.5)
```

```
    f = (1 + 0.3 * (gamma - 1) * M**2)**(-0.12)
    C_f = C_f * f

K_DF = (C_f * S_wet) / (2*d**2)

###############################################################
# Total drag coefficient:
# Cd = K_DC + K_DB + K_DW + K_DF + K_DI
# No data to approximate K_I - we can assume it's small

K_D = K_DC + K_DB + K_DF + K_DW

Cd = K_D / 0.3927

# End of script
```